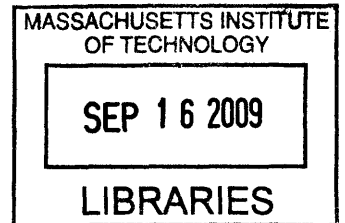**Design and Control of a Robotic Thumb Using Piezoelectric Actuators**

by

Jacob A. Levinson

SUBMITTED TO THE DEPARTMENT OF MECHANICAL ENGINEERING IN
PARTIAL FULFILLMENT OF THE REQUIREMENTS FOR THE DEGREE OF

BACHELOR OF SCIENCE
AT THE
MASSACHUSETTS INSTITUTE OF TECHNOLOGY

JUNE 2009

ARCHIVES

Signature of Author:_____

Department of Mechanical Engineering
5/8/2009

Certified by: _____

H. Harry Asada
Professor of Mechanical Engineering
Thesis Supervisor

Accepted by: _____

John H. Lienhard V
Professor of Mechanical Engineering
Chairman, Undergraduate Thesis Committee

Design and Control of a Robotic Thumb Using Piezoelectric Actuators

by

Jacob A. Levinson

Submitted to the Department of Mechanical Engineering
on May 11, 2006 in partial fulfillment of the requirements
for the Degree of Bachelor of Science in Mechanical Engineering

ABSTRACT

Although much more complex and maneuverable than their predecessors, today's anthropomorphic robotic hands still cannot match the dexterity of human hands. While most of these limitations are caused by inadequate sensor and control systems, the use of large, heavy, and stiff actuators can also contribute to dexterity problems. If we expect robotic hands to interact with humans and human objects, joint actuators must allow a compromise of strength and compliance. Piezoelectric (PZT) actuators exhibit a high backdriveability which could facilitate this compromise. Although they have low displacement and force output, they are useful in fine control applications. When combined with a DC motor, PZT actuators can produce precise, delicate movements in robotic hands. To develop the novel DC-PZT hybrid system, the force and displacement capabilities of PZT actuators were first characterized with a simple one degree of freedom system. The data from this characterization was analyzed and used to develop a one degree of freedom thumb using a hybrid DC motor/PZT actuator system. To study system performance, a simple position control scheme was implemented for the DC motor and PZT actuators. The experimental results suggest that current PZT actuators, even when combined with a DC motor, cannot produce enough thumb tip force to mirror the functionality of the human hand. That said, improvements to the actuator could make PZT-actuated hands a future possibility.

Thesis Supervisor: H. Harry Asada

Title: Professor of Mechanical Engineering

Table of Contents

1. Introduction

The human hand is an amazing mechanical device, capable of holding heavy loads, carefully manipulating delicate objects, and grasping in numerous configurations. While manufacturing robots with specialized tasks have specialized end effectors, robots that must interact with people and unknown objects of varying size, shape, and weight throughout the home and larger world need dexterous, yet durable hands. Anthropomorphic designs try to achieve both the aesthetics and dexterity of human hands by mimicking the mechanical structure of joints and tendons. In the last thirty years, many humanoid hands have been designed with these objectives, but none have fully achieved the dexterity of human hands. This section will detail a few selected designs, discuss the general shortcomings of robotic hands, and propose the use of PZT actuators in a new hand design.

1.1 Previous robotic hands

Many robotic hands have been developed since the early 1970s. While their designs range significantly in complexity and aesthetics, they have all sought to replicate the strength, workspace, and dexterity of the human hand. These hands generally fall into three main categories of actuation: hydraulically actuated tendons, DC motor actuated tendons, and direct-drive DC motor joints.

The Utah/MIT hand was a pioneering robotic hand developed in 1984 as a platform for grasp control studies. [1] It was four-fingered with 16 joints and 16 controlled degrees of freedom. In this design, remotely located pneumatic actuators controlled the tendons rotating the joints. These actuators produced an impressive maximum force output at the fingertips of about 7 lbs. The workspace was limited by a

thumb being mounted directly opposed to the fingers. It also included an impressive array of joint position and tendon tension sensors for use in control applications.

The Robonaut hand was designed by NASA in 1999 for interaction with human tools and control panels in space vehicles. It was a five-fingered, 12 degree of freedom hand with joints actuated by cables connected to DC motor controlled lead screws. Extreme efforts were made to mimic the hand size and strength capabilities of the human hand. This design also featured an impressive array of joint position sensors, encoders, and load cells for position and force control [2].

One of the most recently designed robotics hands is the Gifu Hand III. Developed at Gifu University in 2002, it is a five-fingered hand with 20 joints and 16 controlled degrees of freedom. The joints are directly driven by miniaturized servos. Because of the directly driven joint design, position control on the hand is excellent. The miniaturized components are able to output a maximum force of 2.8 N at the fingertips. Like the Utah/MIT hand, the Gifu III was developed as platform to better understand grasping control, with integrated tactile sensor arrays on the fingers, thumb, and palm [3].

1.2 Shortcomings of Robotic Hands

The human hand outperforms all of the robotics hands discussed. While they are able to execute specific tasks in controlled environment, robotic hands lack the versatility of the human hand in interacting with different objects. Tasks that are simple for human hands, like closing doors, present significant challenges to robotic hands. Much of the ineffectiveness of robotic designs steams from inadequate sensor and control schemes. A better understanding of grasping must also be achieved to fully address this issue. However, there are still significant mechanical issues that have not been resolved.

Space constraints are a significant design concern. Many of the robotics hands discussed saved space by using an exterior power source to drive tendons. While this layout is similar to the forearm muscles used to move the fingers, it causes numerous issues in robotic applications. When tendons are routed outside of the hand, they must pass through the wrist joints, which can contract or relax the tendon during movement. These extra forces interfere with hand performance and significantly increase the complexity of the design. To overcome these problems, we must use an actuator that fits inside the space of the hand.

Additionally, whatever actuator source is used must fit on the robot. For example, the pneumatic actuators on the Utah/MIT hand were driven by a large compressor that could not be reasonably be carried by a mobile robot. Because of these problems, it is most desirable to contain all actuators inside the space of the hand.

Another important design concern is the backdriveability of the finger joints. Human hand muscles are flexible, so they are not easily damaged by excessive forces. This compliance is essential for a robotic hand to function robustly in the real world. The Gifu III hand has very stiff joints because of the high gear ratio in the gearboxes. Even simple human grasps, like a hand shake, produce excessive forces that damage the motors in the Gifu III hand. Backdriveability is also useful for grasping delicate objects. An inherent compliance allows for a more flexible force control scheme.

Choosing the right actuator is key to achieving a robust, controllable anthropomorphic hand. All of the actuators mentioned previously failed to meet these goals simultaneously. The miniaturized DC motors of the Gifu III hand are all located within the hand, but do not have the force output and robustness of an actual hand. The

Utah/MIT hand uses pneumatic actuators that have realistic force output and compliance, but requires a complicated tendon routing system to an outside actuator. A small and compliant, yet strong actuator is needed to significantly improve the performance of robotic hands.

1.3 Project Goal

This paper will introduce the use of an innovative cellular piezoelectric (PZT) actuator as a potential solution to the problems outlined in section 1.2. A robotic thumb actuated by PZT will be designed to explore the capabilities of this actuator for robotic hand applications. Specifically this design will focus on addressing the concerns of space, backdriveability, and dexterity. A control scheme will also be implemented for position control of the thumb to determine system performance.

2. Cellular PZT Actuators

The thumb design will focus on successfully utilizing cellular PZT actuators. These actuators have many advantages over more commonly used actuators, but they must be used intelligently to be effective. A comprehensive understanding of piezoelectric materials and the actuator design is essential to properly designing a robotic thumb. This section will examine the function of piezoelectric materials and the capabilities of the piezoelectric actuators. Next it will provide a basic overview and analysis of the experiments used to test the effectiveness of using PZT actuator in robotic grasping mechanisms.

2.1 Piezoelectric Characteristics

Piezoelectric materials behave uniquely because there is coupling between their elastic and dielectric properties. These materials have a crystal structure that can be electrically polarized at room temperature. Because of this physical characteristic, any mechanical stress on the material generates an electric field on the surface. Conversely, when the material is subjected to a voltage, a strain is induced. This relationship can be quantified for any material as

$$S = E \cdot d \tag{1}$$

where S is strain, E is the potential, and d is a material constant. [4] From this equation, we can see that the displacement of the piezoelectric material is proportional to the voltage applied. Piezoelectric materials act like capacitors in electrical systems, so displacement is also proportional to the charge density in the material.

A few natural materials exhibit this behavior (i.e. quartz, tourmaline, Rochelle salt), but man-made polycrystalline ferroelectric ceramics such as barium titanate and lead (plumbum) zirconate titanate (PZT) provide much better performance. The strain experienced by piezoelectric materials is very small (0.1%) but they are able to generate a significant amounts of force. Because of these characteristics, piezoelectric materials are commonly used in both sensor and fine positioning technologies. [5]

When used as a force generator in actuator applications, the piezoelectric material acts like a spring with material stiffness, k_f, and the force output, F, can be described as

$$F = F_0 - k_f d \tag{2}$$

8

where F_0 is the maximum force that can be generated and d is the displacement. This relationship shows that force generation reduces the effective displacement. At maximum force generation, the displacement falls to zero.

Piezoelectric materials also have excellent control capabilities. They exhibit a fast response to input commands, with the upper limit being one-third of the resonance frequency of the system. This high bandwidth allows for high speed control of piezoelectric materials. Also, because there is no backlash as in motors, the resolution of the control is only limited by the noise of the input signal. This can be advantageous in precision control. Despite these advantages, the piezoelectric materials are not perfect. Without a closed loop control system, there is a small amount of creep over time. Additionally, displacement can vary with extreme changes in temperature.
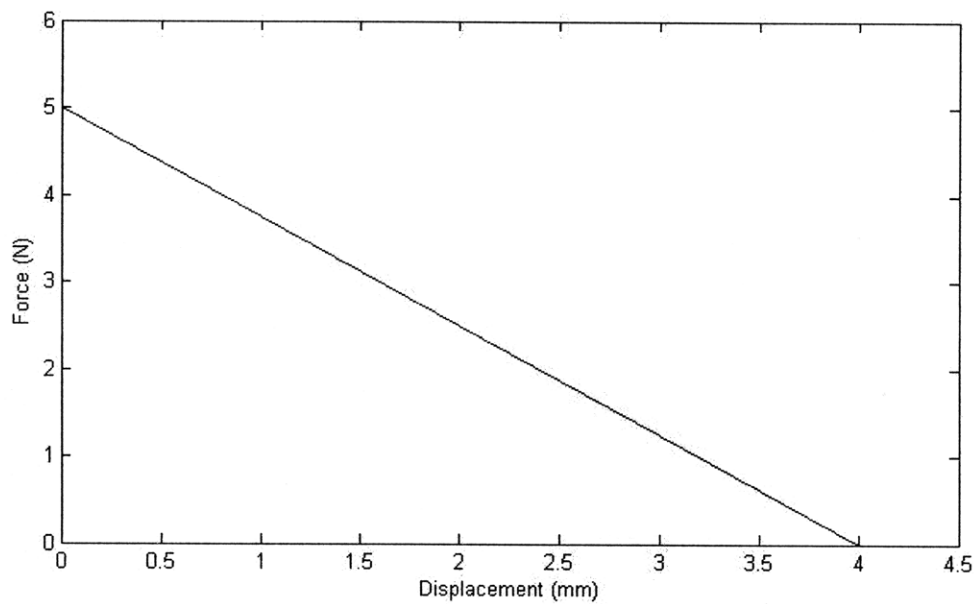
2.2 Capabilities of PZT actuators

Because of the micron scale displacements of piezoceramics, they are normally employed in precision control devices. To be used for contracting tendons in a thumb, the output displacement must be increased to the scale of millimeters. The cellular PZT actuator that is used in this design augments the strains of piezoceramics by using metal flexures to amplify the displacement (see Figure 1). In the cellular PZT actuator, two PZT stacks are enveloped by a steel flexure. This mechanism provides an initial displacement gain of 10. A second brass flexure is attached to the first flexure, providing an additional gain of 10. This effectively increases strain from 0.1% to 10%. The increase in displacement is accompanied by a corresponding reduction in force. Because of non-linearities in the flexure joints, the force output is reduced by a factor greater than 100.
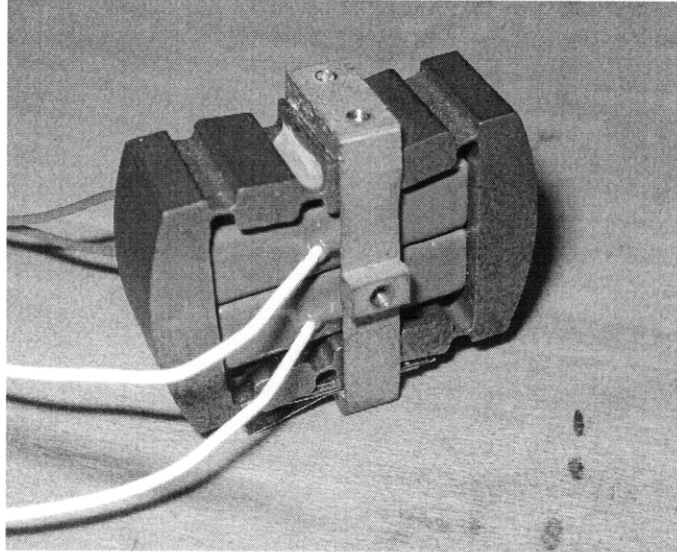
Figure 1. Picture of an assembled PZT actuator cell

For a single actuator cell, the maximum free displacement is 1 mm and the maximum force generated is 5 N. The force generated at a given displacement for these actuator specifications is plotted below using (2). As stated above, this shows that as force increases, displacement decreases.

**Figure 2. Relationship between generated force and displacement.**

One may better understand the capabilities of PZT actuators in robotic hands by comparing their specifications with the functional parameters of human muscles. The strain of PZT actuators is 10%, which is less than the maximum human muscle strain of 40%. Human muscle can put out a maximum stress of 350 kPa, but it can only sustain 100 kPa. A muscle with the same cross-sectional area as the PZT actuator should be able to sustain an output of 75 N. This is much higher than the 5 N output of the PZT. [6] Although PZT is inferior to human muscle in strength and displacement, it still may be able to provide fine positioning and compliance in a hybrid actuated system.

2.3 Experimental Characterization of Cellular PZT Actuators

To properly use the cellular PZT actuators in the thumb design, their performance capabilities were experimentally characterized in an actual system. Because of the low force output and linear displacement expected, it was especially important to ascertain whether they could provide enough force to overcome friction and generate enough displacement to obtain the desired range of motion. These experiments were also able to identify interesting design issues involving actuator orientation and pin routing.

A one degree of freedom thumb testing apparatus was constructed to accomplish these performance tests (see Figure 3). In this design, the thumb rotates around a pin joint connected to the base. A small torsion spring is mounted around the pin to provide a restoring force to the neutral position at 45 degrees. A mechanical stop prevents the thumb from rotating past this position. The cellular PZT actuators are connected to the thumb by a Kevlar tendon attached to another pin. The actuators are held in a mounting container with a screw at the end. This screw allows for easy adjustment of tension in the tendon and actuators. On the base, there is a mounting slot for a load cell for measuring

force at the thumb tip. Pins can be inserted into the base in front of the actuators to test

force losses when routing around pins.
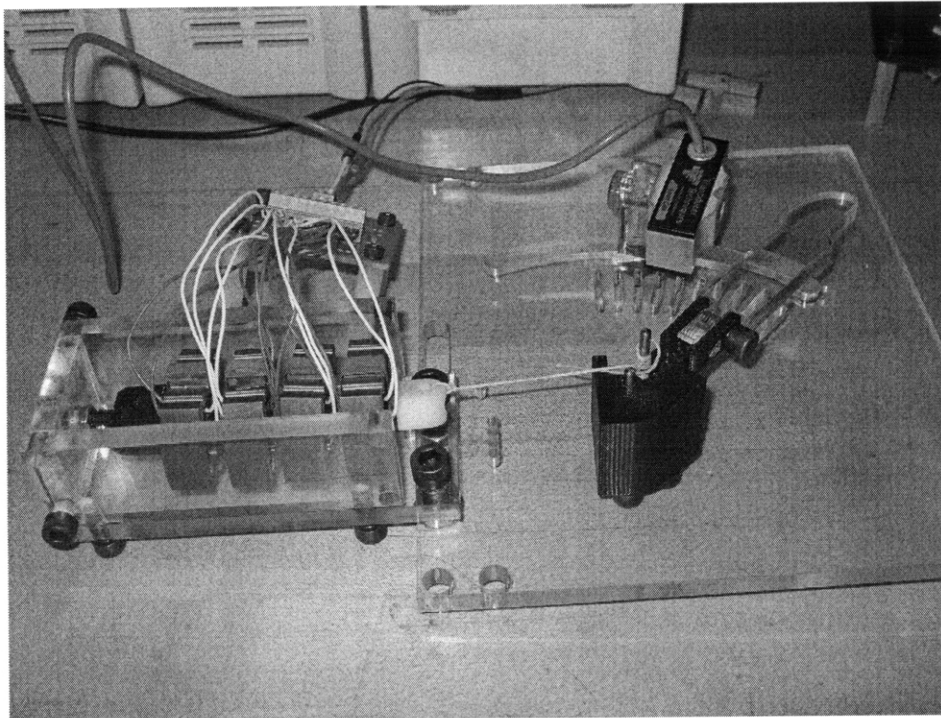
Figure 3. Fully assembled PZT actuator testing apparatus.

2.3.1 Range of motion

Range of motion is an important concern in the prototype design, as the PZT

actuators will need to produce large angular displacements in the thumb. If the PZT is the

only actuator used in the design, it will need to produce at least 45 degree displacements

at the joints to exhibit a realistic range of motion for the thumb. A geometric analysis of

the experimental apparatus can show the relationship between linear displacement and

joint angle (see Figure 4).
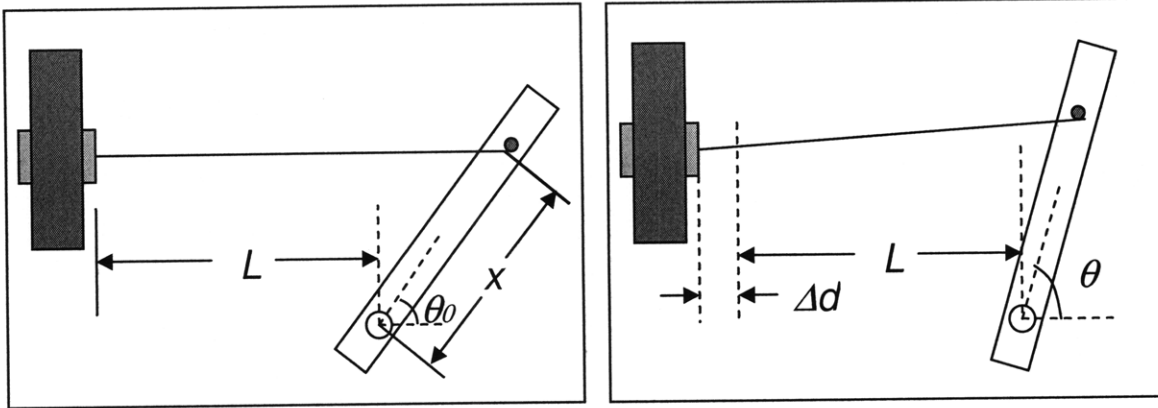
Figure 4. Geometry of the pin joint with tendon attached; initial configuration (left) and final configuration after rotation through angle θ.

Because of the fixed radius of the attachment pin, the tendon will angle slightly

upward as it rotates. This leads to nonlinearities in the relationship between tendon

displacement and joint angle. This relationship can be calculated from the geometry of

the system. The initial tendon length is 45 mm for the apparatus. The initial angle, theta,

is 45 degrees. The distance between the joint and the thumb attachment point, x, can be

varied, but was chosen to be 5 mm for these experiments. This was the closest that the

attachment point could practically be placed to the pin joint. An attachment point farther

from the pin joint would allow for a greater force output but would have reduced the

effective range of motion.

From the geometry of the system, the actuator displacement required to achieve

any angle is given by,

$$\Delta d = x\left(\cos\theta - \cos\theta_0\right) \tag{3}$$

Using this equation, we can see that for a change in angle of 45 degrees, the necessary

change in tendon length is 3.5 mm. If we assume a free displacement of about 1 mm for

each cellular PZT actuator, then a four actuator setup seems like it would be able to

achieve the desired range of motion. Unfortunately, the expected displacement was not

13

observed during testing. The experimental data indicates that four PZT actuators can only produce an angular displacement of 25 degrees and a linear displacement of 2 mm. The forces on the actuators during operation account for this discrepancy. As depicted before in Figure 2, with greater forces acting on the actuator, the potential displacement decreases. Clearly, the force production and displacement of the PZT actuators need to be considered together during the design process.

2.3.2 Blocking Force

The blocking force at the thumb tip corresponds to the pinching force output of the cellular PZT driven hand. Maximizing this force will be important in the design stage, so all of the forces acting on the system need to be understood. The tip force at any angle can be found by performing a torque balance on the system (see Figure 5).

$$\sum \tau = \left(F_{act} + T \right) r - \tau_{spring} - F_{tip} R = 0 \tag{4}$$

The force of the actuator will decrease with increasing displacement as described in (2) and Figure 2. It will also be reduced by the amount of tensions acting on it. This relationship can be described by

$$F_{act} = F_0 - kd - T \tag{5}$$

14
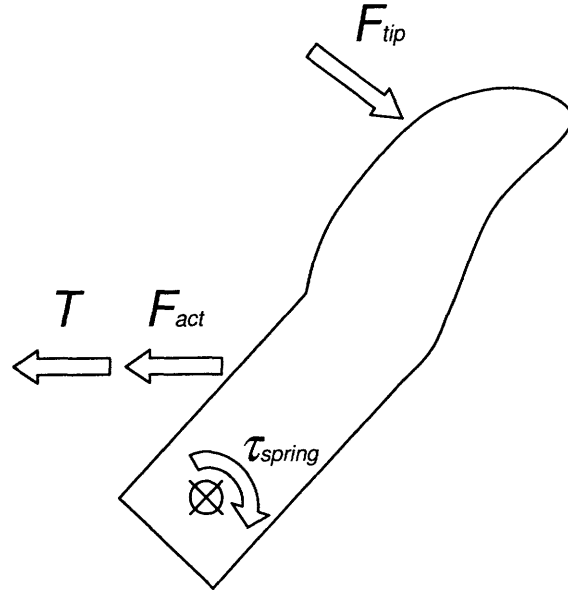
Figure 5. Free body diagram of forces and torques acting on the thumb in the testing apparatus.

The spring torque is defined by a constant torsional stiffness, k_{spring}. The torsion spring was bent slightly beyond 180 degrees, so this initial torque must be also be added to the system. To account for this extra torque, we must write the equation as follows

$$\tau_{spring} = k_{spring}\left(\theta + \theta_0\right) \tag{6}$$

The tension in the system was adjusted to counteract the initial torque of the torsion spring on the system. This initial tension is necessary to keep the tendon taut, so that no actuator displacement is lost due to slack. It can be defined as

$$T = \frac{k_{spring}\theta_0}{r} \tag{7}$$

Knowing equations (5), (6), and (7), we can plug them in to (4) and then rearrange the terms to define the force at the thumb tip, F_{tip}:

$$F_{tip} = \frac{\left(F_{tip} - T - kd\right)r - k_{spring}\theta}{R} \tag{8}$$

15

Because we have values for all of these variables, this model may be used to predict the force output at the thumb tip.

An experiment was conducted measuring the force output at different angles (see Figure 6). With no displacement the blocking force was 0.125 N. At 20 degrees the blocking force drops to zero and the thumb cannot rotate any farther. This corresponds to a maximum actuator force of approximately 3 N and a free displacement of 3.19 mm. The experiment showed a relatively low maximum tip force, but this was predicted by the model. Tension clearly has a negative impact on the system performance, but this tension is required to return the thumb to the neutral position without adding an extra actuator.
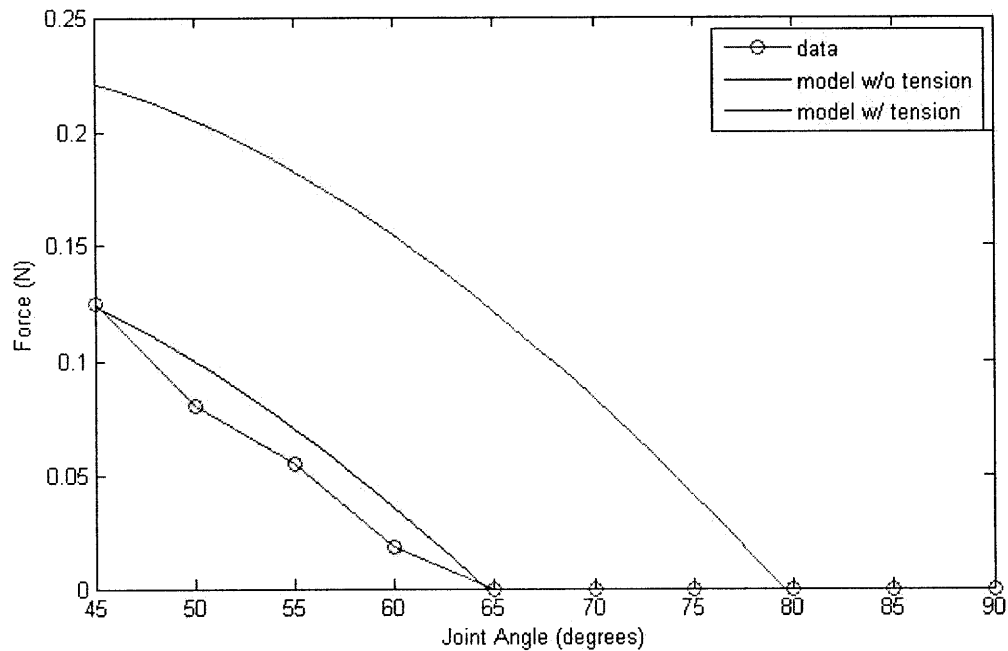
Figure 6. Thumb tip force on the testing apparatus at different joint angles.

There are some differences between the model and the experimental data that could be explained by a number of different factors. For example, the actuator end of the tendon is not fixed as assumed in the model, so it probably shifts slightly during movement. Also, joint friction could reduce the force output. The model itself may be

slightly inaccurate due to physical parameter variability, such as a lower-than-specified

torsion stiffness. Overall, the model provides an accurate prediction of actuator

performance.

2.3.3 Pin Routing

Routing tendons to the joints in the finger requires that the tendon passes around

pulleys or pins in the system. Because a pulley routing system is complicated to design

and assemble, we elected to investigate the reduction in force output that comes from the

simpler method of routing around pins. The capstan equation describes the reduction in

force when a rope passes around a post,

$$T_2 = T_1 e^{\mu\beta} \tag{9}$$

To estimate this reduction for the thumb design, a simple example system with a tendon

in contact with two steel posts for 90 degrees (β) can be used (see Figure 7). This would

allow for two 90 degree changes in direction during routing, which might be necessary in

a two degree of freedom design. The friction constant for steel on Kevlar (μ) is about 0.2.
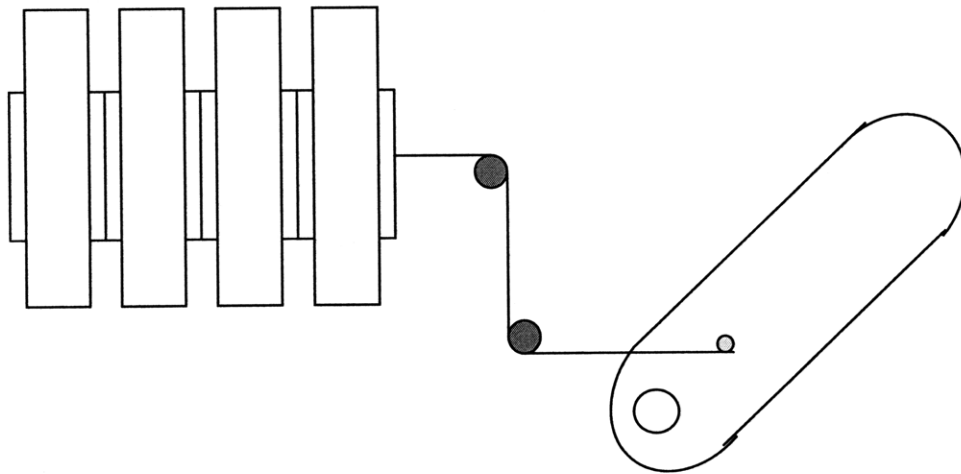
Figure 7. Top view of example routing configuration. The tendon changes direction by 180 degrees while in contact with the steel posts.

With these values, we can calculate the loss in force around each post. Around the first post, the force is reduced from 5 N to 3.65 N. Around the second post, it is reduced further to 2.65 N. This is a predicted force loss of 27% at each post, and a force loss of 47% overall. Because of the already low force output of this system, these types of losses would be incredibly detrimental on system performance.

Experiments confirm this theoretical force reduction. The PZT actuator displacement is linearly related to the force output by (2) so it was used a simple indicator of force losses. Displacement (in degrees of rotation) was measured for 3-5 PZT actuators both with and without routing (see Figure 8). While there was some variation in angular rotation because of different pre-tensions in the tendon, the pin routing system clearly reduced for by 50 to 70%. This is higher than the predicted values, probably due to misalignments in the system and frictional effects at the pin joint and the actuator mount.
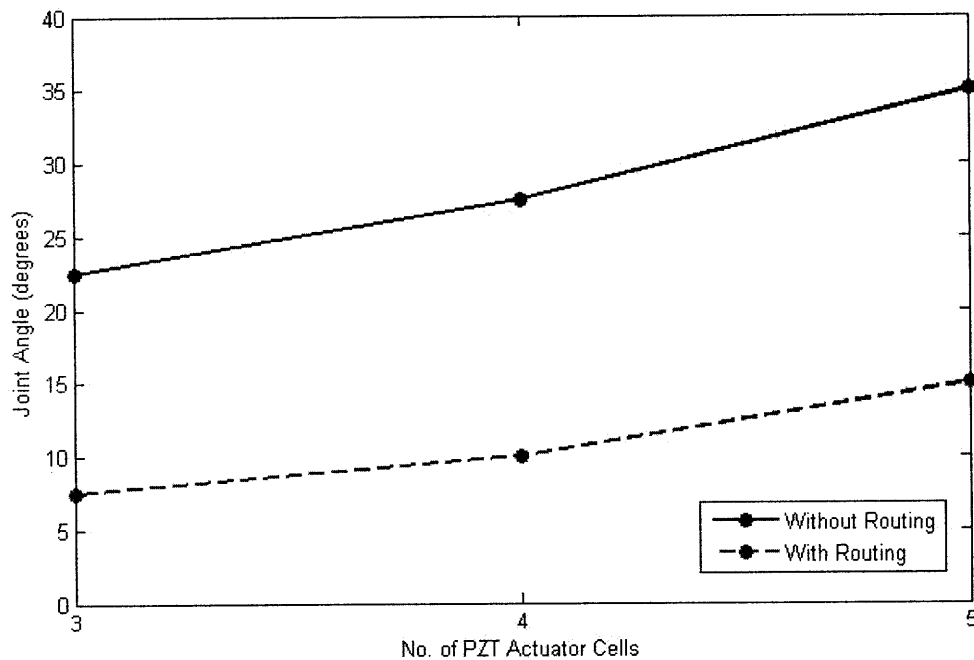
Figure 8. Plot of average joint angle rotation versus number of cellular PZT actuators for routing and non-routing conditions.

2.3.4 Orientation

The prototype was designed so that gravity would not have an effect during most testing. However, in actual operation the human hand must function in many orientations. The PZT actuator string will also be subject to changes in orientation, so it is important to test how different configurations effect the operation of the PZT actuator.

Looking again at a simple force body diagram, we can balance the torques on the system, with gravity now included. Because of the low force output spec of 5 N from the PZT actuators, the torque from gravity, even on a light plastic thumb, is on the same order of magnitude. Intuitively, this would suggest that the PZT actuator will perform differently. In the upward orientation, where the thumb is working against gravity, the thumb will likely rotate through a smaller range of motion. In the downward orientation, where the thumb is working with gravity, it should be able to rotate through a greater range of motion.

Experiments with the free displacement of the PZT actuators substantiate this belief. In the upward orientation, the thumb was only able to rotate through 5 degrees. In the downward orientation, the thumb could rotate through the whole 45 degrees, but the thumb actually sagged 15 degrees from the neutral position.

This inability to maintain the neutral position is largely due to the torsion spring not having enough torque to support the thumb's weight. However, it also is due in part to an increase in tendon tension from the weight of the PZT actuator. When oriented vertically, the mass of the PZT actuator cells adds an extra force to the system and contracts the tendon more than desired. Because of the weight of the PZT actuator cells, this force may actually exceed the force output of the actuators. The same problem occurs

in the upward orientation. This data suggests that PZT actuators are not controllable in different orientations. This problem with controlling tension is a serious issue that must be considered in future PZT actuated hands.
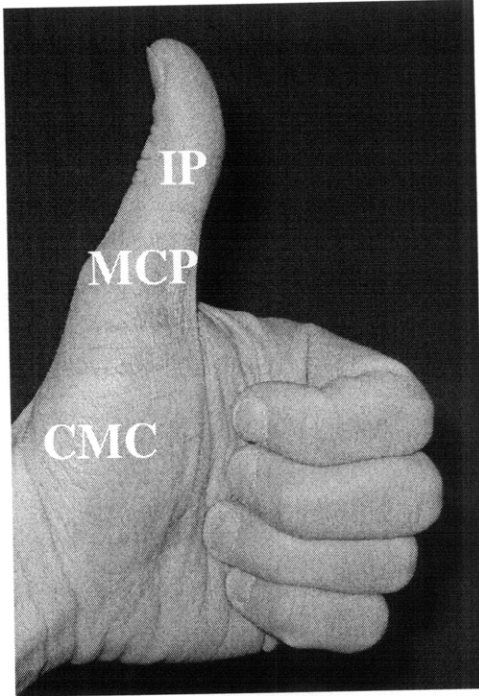
2.4 Observations

These tests have uncovered characteristics of the PZT actuators that will be helpful in design. A large range of motion is not realizable because the actuators produce small displacements, even with only small forces acting on them. Low force output will also cause problems in design. These tests show that these actuators cannot provide a realistic human thumb tip force by themselves if they are required to rotate through a large range of motion. Even at smaller ranges of motion, the force output will not be able to match human thumb tip forces. Tendon routing should be minimized because it decreases the force output significantly. Additionally, orientation will likely have a serious effect on performance no matter which design is chosen. Overall, future PZT actuated designs must consider the force output and displacement of the PZT actuators. This will be necessary to optimally use these actuators in robotic hand application.

3. Design Considerations

Designing an anthropomorphic thumb requires the integration of several mechanical and aesthetic details. This section will describe the functionality of the human thumb, outline design goals, explore the merits of a few design options, and then detail the design of the selected option.

3.1 Requirements

To be considered truly anthropomorphic, the robotic thumb should have motions and force outputs similar to the human thumb. The human thumb consists of three bones and has three joints, which are controlled by muscles in the hand and forearm. The interphalangeal (IP) is a hinge joint with 90 degrees of rotation. The metacarpophalangeal (MCP) is also a hinge joint but its range is only 10-50 degrees. The carpometacarpal (CMC) joint at the base of the thumb is a saddle joint, which has two degrees of freedom. The radial adduction/abduction motion (movement from the edge of the palm by spreading the thumb outward) has a range of 60 degrees. The palmar adduction/abduction motion (movement of the thumb away from the surface of the palm) has a range of only 45 degrees. The CMC joint allows the thumb to oppose the other fingers. The muscles that control palmar abduction and adduction are located in the palm, but the rest are located in the forearm. In precision pinching grips, these muscles exert a maximum force of 80-120 N, but it is estimated that a force of 10 N is sufficient for most daily activities. [7]

Figure 9. Human thumb with joints labeled.

This design will be focused on the pinching motion of the thumb, so the prototype joints should be able to replicate this motion. The natural joints would be difficult to imitate directly. The motion of the MCP saddle joints is especially complex, but it can be

approximated with a rotational joint and an abduction/adduction hinge joint. Whatever joints are used should be able to rotate through 90 degree to pinch the index finger. Ideally, the thumb will produce a pinching force of 10 N. If this is not possible, the design should maximize this pinching force. The speed of response should also match that of a human hand. The size, weight, and aesthetics must be comparable as well.

This design should also address the concerns raised earlier in relation to previous robotic hands. The joints must have some backdriveability, so they will not be damaged easily. Also, all the actuators driving the thumb must fit in the palm of the hand to reduce complexities that occur when routing tendons through a wrist.

3.2 Design options

To meet these requirements, there are two main options. One is to use the PZT actuators to directly drive the smaller range of motion movements, in the IP and MCP joints, while a DC motor drives the larger range of motion. The scope of this project would limit the design to a two degree-of-freedom PZT actuated thumb. This design accomplishes the backdriveability objectives, but it has other limitations. Given the experiments on range of motion, pin routing, and the constraints on space, this design would only be able to rotate through about 10 degrees at each PZT driven joint. Additionally, the maximum force output at the thumb tip would be very small, on the order of 0.05 N. This does not meet our anthropomorphic design requirements and would not have a particularly impressive performance overall.

The second option is to use a hybrid system, where a DC motor and PZT actuator drive the same thumb joint in parallel. The DC motor could provide the large scale range of motion, while the PZT cells provide fine positioning control. One clear benefit of this

design is that the PZT actuators will be able to provide much more force at the thumb tip because of the reduced range of motion. It will also still have compliance over the range of the PZT actuator. However, there are potential space concerns because now two actuators are driving one joint. This could be resolved in the future by using a synergistic design where the motor drives multiple tendons attached to different diameter pulleys and PZT actuators drive fine motion on those joints.
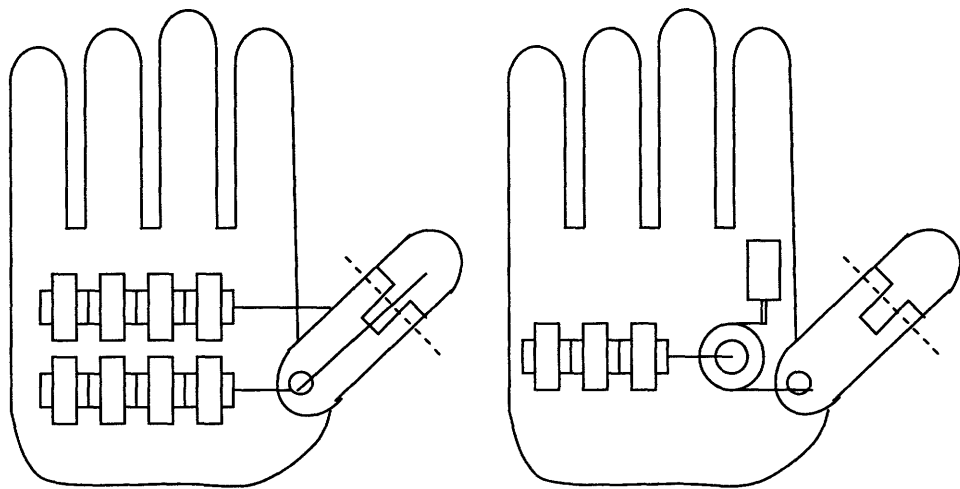

Figure 10. Potential design implementations: PZT actuator driven (left), hybrid DC motor/PZT actuator(right).

Ultimately, the second design was chosen because it has a greater chance of accomplishing the anthropomorphic design requirements, especially for the desired range of motion and force output.

3.2 Mechanical Design

The main focuses throughout the design process were simplicity and ease of manufacturing. In the final design, all of the actuators and components are mounted on an acrylic palm which is oriented vertically. The palm has "knuckles" to allow for the insertion of fingers. An acrylic index finger was created that has pin joints and is held in place by friction. The joints can be positioned at any angle, and the finger provides a

somewhat realistic pinching surface for the thumb. The thumb joint is a simple vertical pin joint on the palm which allows the thumb to rotate in the z-axis to touch the index finger. A torsion spring is mounted inside of the joint. While the torque that the torsion spring generates reduces the possible force and displacement of the system, it is necessary to maintain tension in the tendon and return the thumb to the natural position without adding another actuator. The thumb is also made of acrylic and maintains the correct size and weight.
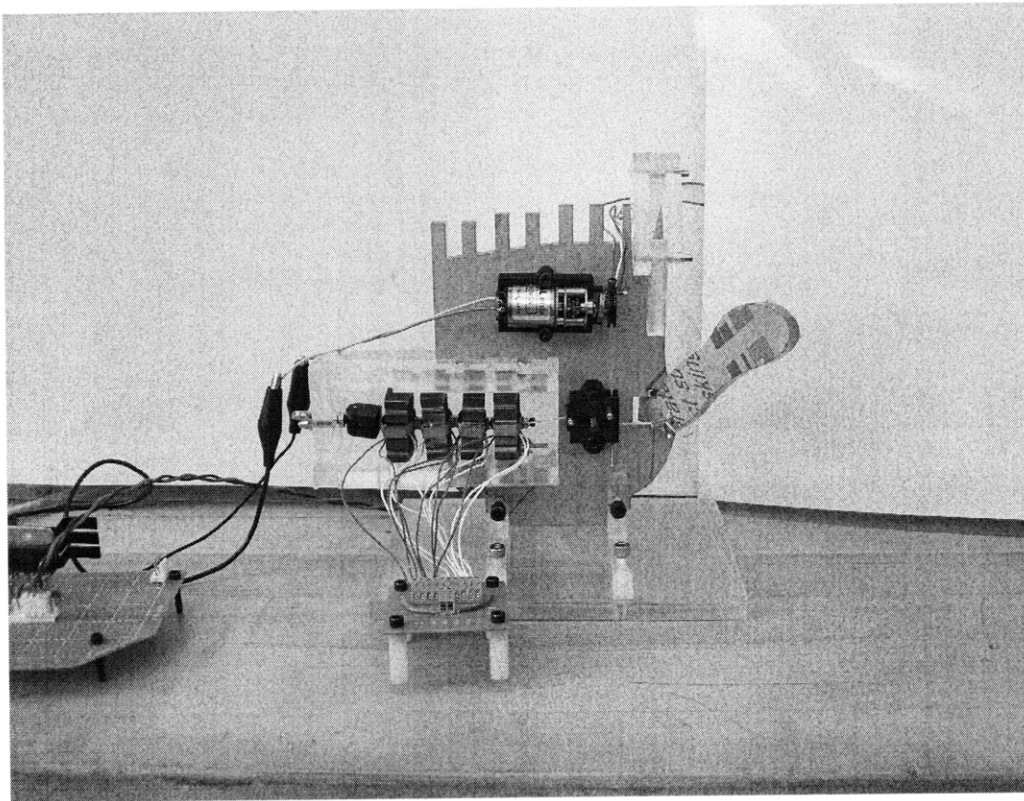

Figure 11. Front view of fully assembled hybrid DC motor/PZT actuator prototype.

The cellular PZT actuators were mounted in an acrylic chamber attached to the front of the palm. The container only allows for 0.05 inches of vertical movement, which restrains the actuators from sagging under their own weight. This minimizes any displacement losses in the actuator string. A wing nut was attached to the back end of the container so the tension could be easily adjusted during operation. In this initial iteration,

the PZT container does not fit into the body of the palm, but the container was purposefully oversized to allow reconfiguration of the number of actuator cells in this prototype. With a more compact container and attachment design, at least four PZT actuators would be able to fit into the body of the palm.

The DC motor is mounted on a 3D printed enclosure attached to the palm. Size was the most important concern when choosing this motor. Because the motor is so small, it can fit into the surface of the palm. A surface mount potentiometer fits around the shaft for use as a simple angular sensor for position control. The enclosure contains a small slot to constrain the potentiometer during operation. A pulley is attached to the motor shaft with a set screw. This pulley is connected to a tendon, which leads to the tendon routing mechanism.

The routing mechanism is the most complex and important part of the hand design (see Figure 12). On the interior of the part, a small pulley sits around a steel pin in a guide shaft. In the neutral position this sits at mechanical stop at the end of the shaft. The tendon from the DC motor passes around a routing pin, wraps around this pulley, passes around another routing pin and attaches to the thumb. The tendon from the PZT actuator is connected to the pulley by a small 3D printed piece.
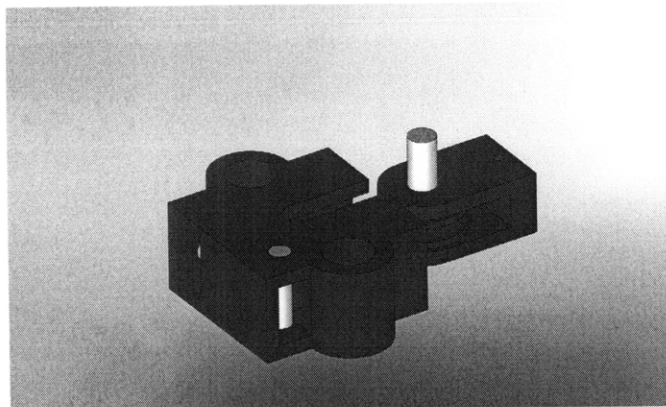
Figure 12. 3D model of tendon routing mechanism.

25

Because of the pulley system, the DC motor and PZT actuators are able to act in parallel. The tendon from motor is routed around the pulley and its displacement can rotate the thumb through the entire desired range of motion. The PZT actuator pulls the entire pulley assembly down the guide shaft. Because the tendon wrapped around the pulley is fixed at the DC motor, the displacement of the actuators is magnified by two. This magnification is advantageous for minimizing the number of cells required. However, this same arrangement also doubles the force acting on the PZT actuators. This could potentially over-tension the tendon reducing performance, but the mechanism was designed so that the initial state of the pulley is at the back stop of the guide shaft. This reduces the load on the PZT actuators. Additionally, the pulley rotates with very low friction so that almost no energy is lost to friction.
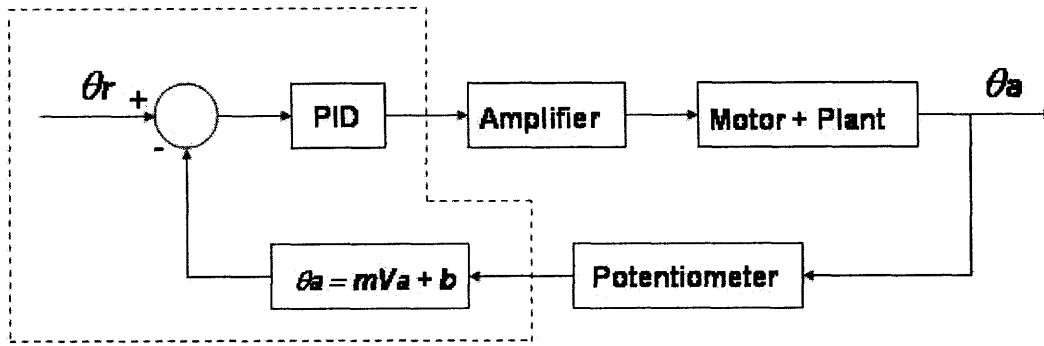
4. Controls

As discussed in the introduction, grasping control schemes are essential for achieving the dexterity of human hands. This requires accurate sensor data to control position and force output of the joints. While this project does not attempt this scope of intelligent controls, it will implement a simple position controller on both the DC motor and PZT actuators to investigate the performance of the system. This section will also investigate the potential use of PZT actuators as a force sensor for force control.

4.1 DC Motor Controls

The DC motor needs to be able to rotate through a full 90 degree range of motion and be positioned at a desired angular value. In order to accurately perform position

control with the DC motor, a closed loop feedback controller was implemented. The

block diagram in Figure 13 identifies all of the components in the control system.

Figure 13. Block diagram for position control of the DC motor. The dotted line contains the reference input and control blocks that were implemented in LabVIEW.

The reference angle is defined by the user in LabVIEW software and sent to a

controller which adjusts the signal and converts the output voltage into an analog signal.

The amplifier outputs an increased voltage to the motor causes the motor shaft and the

joint angle. The potentiometer measures the shaft angle and sends this back into

LabVIEW where it is converted to an estimated angle with a relationship between angle-

voltage. The error signal is sent back into the control loop to adjust the system.

The linear relationship between angular displacement and voltage output of the

potentiometer was experimentally determined from the system by reading the voltage

output at known angles. This allows a conversion of the potentiometer measurement back

into the actual joint angle in the feedback loop. The slope of the linear fit was constant

across calibrations, but the offset must be recalibrated whenever the tendon is adjusted.

While this linear fit is convenient, it is important to make sure that this

assumption will not cause significant positioning errors during operation. An analysis of

the joint kinematics can yield the actual relationship between joint angle and tendon

displacement (see Figure 14).
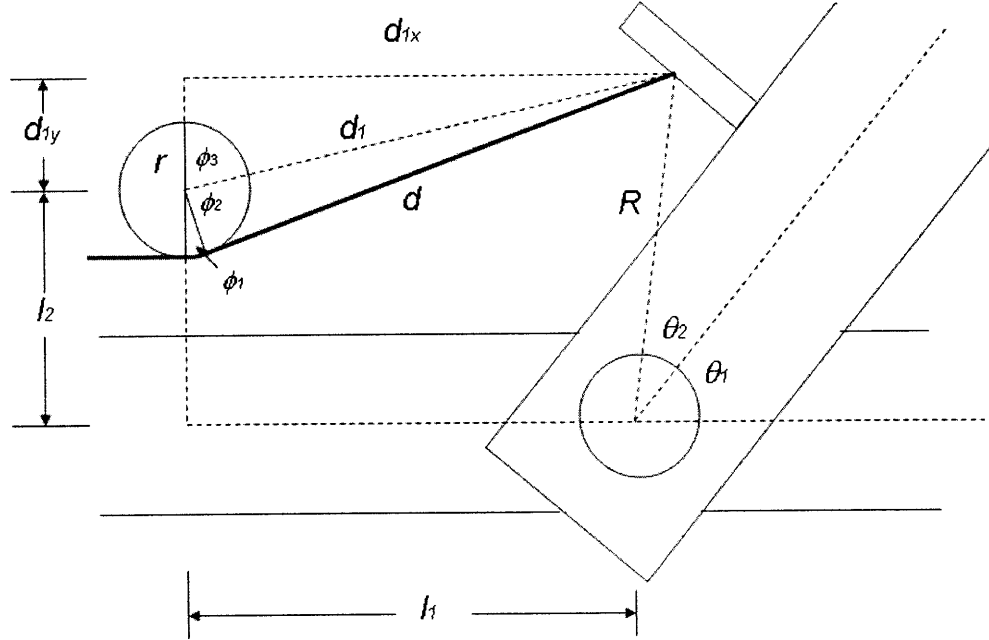
Figure 14. Geometry of the thumb joint, tendon, and routing pin for the prototype.

At any joint angle, the tendon length is defined as:

$$L = d + r\phi_1 \tag{10}$$

The dimension of r is defined by the system, but d and ϕ change with the joint angle. The

length of d can be calculated from the equation

$$d = \sqrt{d_1^2 - r^2} \tag{11}$$

Now, we must calculate the length of d_1

$$d_1 = \sqrt{d_{1y}^2 + d_{1x}^2} \tag{12}$$

The x and y components of d_1 will change with the joint angle θ_1 by the following

equations:

$$d_{1y} = R\sin(\theta_1 + \theta_2) - l_2 \tag{13}$$

28

$$d_{1x} = R\cos(\theta_1 + \theta_2) + l_1 \tag{14}$$

By plugging (13) and (14) into (12) and then (12) into (11), we can solve for the length of

d. The tendon length is also dependent on ϕ_1, which can defined by angles ϕ_2 and ϕ_3 so

that

$$\phi_1 = \pi - \phi_2 - \phi_3 \tag{15}$$

These angles are defined by the geometry of the system and can be expressed as:

$$\phi_2 = \cos^{-1}\left(\frac{r}{d_1}\right) \tag{16}$$

$$\phi_3 = \tan^{-1}\left(\frac{d_{1x}}{d_{1y}}\right) \tag{17}$$

By plugging (16) and (17) into (15), the magnitude of ϕ_1 is now defined. With these

outcomes, we can now solve for the tendon displacement at any joint angle. The resultant

equation is too long to write out explicitly here, but the results are plotted in Figure 15.
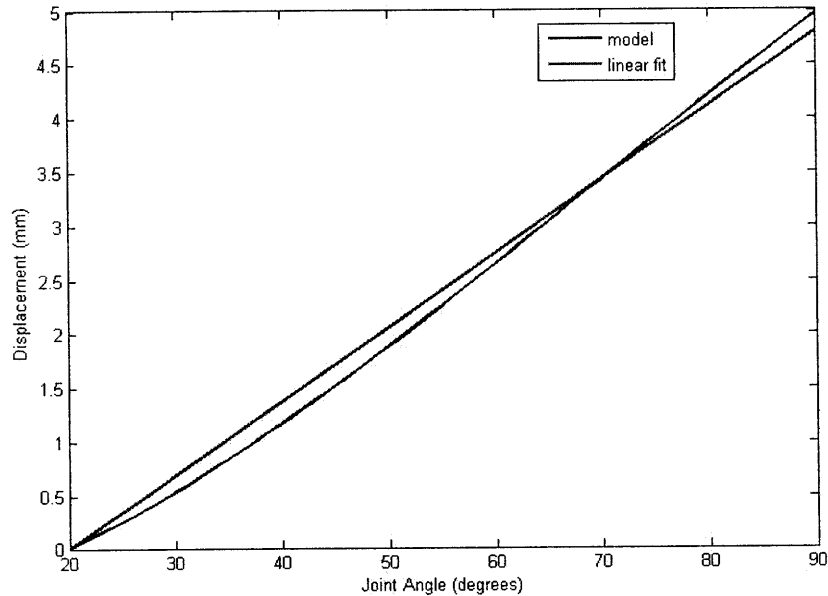
Figure 15. Plot of linear displacement versus joint angle for the actual relationship (blue) and the linear estimation (green).

29

From Figure 16, it can be seen that the errors from using a linear model are less 3 degrees for the entire 70 degree range of motion. This conclusion means that this model is valid when high positioning resolution in not essential. A higher order fit could be used if more accurate positioning was necessary. This same kinematics analysis would need to be done for more complex routing geometries in a multiple degree of freedom thumb where coupling could play a significant factor.

The actual controller was implemented in LabVIEW using a pre-made PID block. Control parameters were estimated utilizing an iterative design process. Without any control, the system exhibited overshoot of the desired angle. For example, when moving from 25 to 85 degrees, the thumb would actually overshoot so much that it hit the index finger. Even these small of overshoots of 3-5% are not desirable when grasping delicate objects. There is also a small steady state error of 0.7 degrees without any control. The settling time is 0.1 sec, which is an appropriate response time for a hand. First, changing the proportional gain was used to try to correct the system. For a gain of K = 0.5, the system no longer exhibits overshoot but the steady state error increases to 1.2 degrees. The settling time also increases slightly to 0.075. This is somewhat of an improvement on system performance. Any lower gains will slow down the system response and increase the steady state error significantly (see Figure 16).
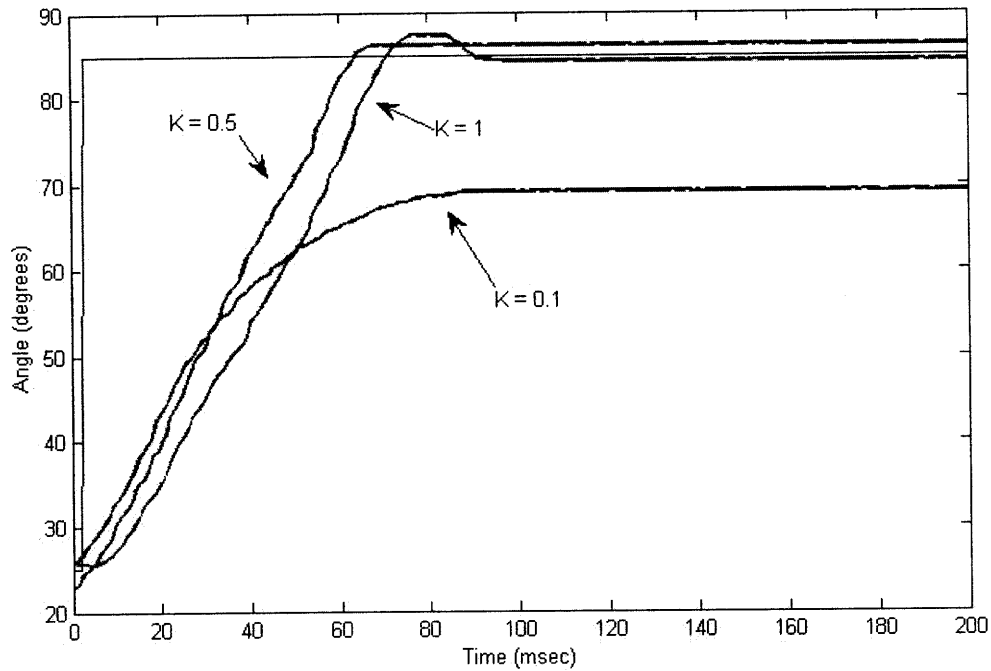
Figure 16. Time profiles of joint angle to a step reference input of 85 degrees for different proportional controllers.

To get rid of the steady state error, an integrator was added to the system next. An initial integrator of 0.4 was chosen. It slowed down the system significantly, but unexpectedly, the integrator caused the system to overshoot. It also caused an effect where the system would never settle to the desired angle but would continue to adjust on either side. This problem is likely due to stiction in the joint. The integrator accumulates the error until it can move, but then forces the system to overshoot by 1 degree. This periodic adjustment would have a negative impact on any attempts to grasp objects. Efforts to solve this problem physically by adding lubricant to the joint and pulley were unsuccessful. Implementing anti-windup or deadband in the controller could potentially be used to solve these problems in the future.

Attempts to use derivative control to speed up the system response were
unsuccessful. At higher gains, it amplified noise in the system causing unwanted chatter
in the motor gearbox. At lower values, it had no apparent effect on the system.

This process identified proportional control as ideal for this case because of the
periodic over-adjustment by the integrator, but a system with a proper integrator would
be ideal for completely eliminating error. To implement a highly accurate control system,
it would be better to identify the system parameters rather than by simply adjusting the
PID gains. This was not done on this project, but would be possible if desired.

4.2 Cellular PZT Controls

In addition to controlling the DC motor position, fine positioning of the PZT
actuators is needed for performing delicate grasping tasks. As discussed previously, the
voltage across piezoelectric materials and their displacement are directly proportional. By
determining this relationship, it was possible to use an open loop controller to position
the PZT actuator. Experimentally measuring the change in joint angle at the minimum (0
V) and maximum (150 V) voltages, a range of motion of approximately 10 degrees was
found. If we assume that this relationship between joint angle and voltage is linear, we
can now perform the open loop control by simply inputting a desired voltage in software.
As with the DC motor the geometry of the system does lead to some non-linearities, but
these nonlinearities will only lead to small errors. A more precise calibration could be
performed if desired. This open loop control allows us to finely position the thumb.

One intriguing aspect of PZT actuators is their potential for dual use as a force sensor
and an actuator. This project was not able to experiment with this innovative capability,
but it will discuss the theory because it represents an advantage of PZT actuation. Any

force on the PZT actuators, stresses the piezoceramics, and generates electric charge. There is a linear relationship between the force applied and electric charge generated, which makes this a convenient and accurate load cell. By recording the charge on an actuator cell, we can directly measure the force on it. There are two main implementations of this idea. In the first case, one cell in the actuator string could be used solely as a sensor. Alternatively, one PZT actuator cell could serve some dual role as a sensor and actuator. This might operate in some timeshare mode, where the charge on the PZT stack is measured at higher frequencies for only a split second. In both cases, there are limitations.

Piezoelectric load cells are used in industry, but they typically only measure dynamic loading. The relative change in electric charge is apparent for impacts, but the load cells fall out of calibration easily because the very act of measuring the voltage causes charge to leak off of the piezoelectric transducer. If we are trying to measure static loads for force control, this represents a serious problem. One potential solution is to use a high impedance measuring source, such as a charge amplifier. The charge amplifier produces an output proportional to the charge, and significantly reduces charge leakage. These quasi-static measurement are excellent, but literature suggests that even with a charge amplifier long term static output is not practical [8]. It may be possible to circumvent this issue by resetting the PZT sensor at a known force during operation. This could be as simple as resetting the sensor when the thumb is at its neutral position. By recalibrating the thumb continually, the quasi-static measurements may be good enough for practical use. Additional issues would be involved with a timeshare mode. The measurement time would need to be short enough to not disrupt the desired actuation time and to not allow

charge leakage during measurement. Considering the high bandwidth of the PZT

actuators, this may be achievable. These and any other issues could be further resolved in

experimentation.

4.3 Overall Performance

For the final prototype, the range of motion is 90 degrees, with the DC motor able

to rotate through the entire range and the PZT actuators having a 10 degree range. The

positioning accuracy with the current control scheme is ±3 degrees, but could be further

resolved with better calibration. The force output at the thumb tip is now approximately

0.35 N. This force is enough to hold up small, light objects such as paper clips and

straws.
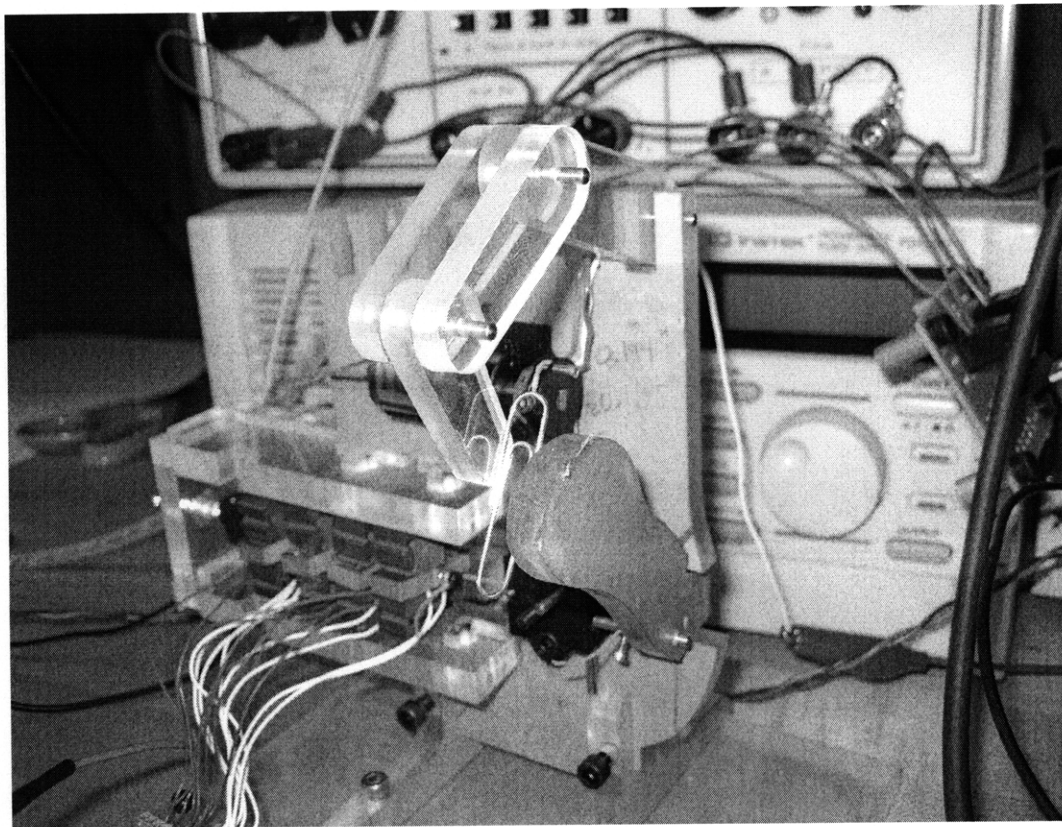
Figure 17. Thumb prototype pinching a paperclip.

Increasing the friction at the fingertips would allow the prototype to hold even heavier objects. The compliance of the PZT actuators enables it to hold delicate or deformable objects without exerting excessive force on them. As expected, orientation still has a significant effect on the system performance. The weight of the PZT actuators contracts the tendon when the thumb is working with gravity. When moving against gravity, the thumb can only displace 5 degrees. This issue will need to be resolved in future implementations.

5. Conclusions

The hybrid DC motor/PZT actuated thumb was a successful implementation of the design goals. While it is hard to quantify the actual grasping capabilities without more complex control systems, the thumb was able to perform anthropomorphically in many ways. The accomplishments of this project and suggestions for future work are outlined in this section.

5.1 Accomplishments

A robotic thumb was designed that successfully utilizes a hybrid DC motor and PZT actuator drive system to actuate through a 90 degree range of motion. In many regards, the prototype met the anthropomorphic design parameters. The final size of the design is comparable to the human hand with palm dimensions of 95 mm by 130 mm and a depth of 35 mm. The prototype has an overall weight of approximately 0.46 kg. The speed of response was close to 0.1 seconds, which is similar to human muscle capabilities. However, the thumb tip force of 0.35 N was not close to the 10 N threshold

set for practical use. This is a limitation caused by the low force output of the PZT actuator. With improved actuator characteristics in the future, this issue may be resolved.

The DC motor was controlled with a closed loop controller to achieve relatively accurate position control over large ranges of motion (±3 degrees). The PZT was used for fine motion and delicate pinching by implementing a simple open loop control.

5.2 Future work

To truly match the capabilities of the human thumb, there is much more work to do on this design. The next stages of this project should focus on increasing the degrees of freedom in the thumb design, exploring the force sensing capabilities of the PZT actuators, and addressing issues with orientation. The current hybrid system is not expandable to a multi-degree of freedom thumb because of space constraints. A synergistic design could use one DC motor to complete the large range of motion for all joints and a set of PZT actuators to control fine joint motions. [9] This would require additional routing, but given the current system's success despite routing, it should not be a huge concern.

The dual actuation/sensing potential of the PZT actuators should be fully explored. These integrated sensing capabilities are a real benefit over existing actuators, which must rely on external sensors. Experimentation should focus on static force sensing, which will be necessary for force feedback in grasp control. The hardware outlined in section 4.2 should be built and tested. Additionally, the rate of charge leakage should be established to understand how often automatic recalibrations need to occur.

The effect of orientation on system performance is a huge concern that has gone largely unaddressed in this design. The PZT actuators need freedom to move linearly, but

this same freedom allows them to weigh on the tendon in different orientations. Perhaps some sort of mechanical stop system could be devised to eliminate this issue. Future work will have a large impact on the feasibility of PZT actuator use in robotic hands.

5.3 Final Remarks

A hybrid DC motor/PZT actuated thumb was successfully designed and constructed. This actuation system does not match human force output capabilities with the current technology, but with improvements in PZT actuators, it could become a more realistic solution. Future work on the force sensing capabilities will further establish the viability of PZT actuators in robotic hand applications.

6. References

[1]   Jacobsen, S., Iversen, E., Knutti, D., Johnson, R. and Biggers, K. "Design of the Utah/MIT dextrous hand." Proceedings of the IEEE International Conference on Robotics and Automation, ICRA 1986.

[2]   Lovchik, C., Diftler, M. "The Robonaut Hand: A Dextrous Robot Hand for Space." Proceedings of the IEEE Internation Conference on Automation and Robotics, Vol. 2, pp 907-912, Detroit, Michigan, May 1999.

[3]   T. Mouri, et al. "Anthropomorphic Robot Hand: Gifu Hand III", Proceedings of the International Conference on Control, Automation and Systems, October 2002.

[4]   Arnau, Antonio. *Piezoelectric Transducers and Applications*. Springer-Verlag: Berlin, Germany, 2004.

[5]   "Designing with Piezoelectric Transducers: Nanopositioning Fundamentals." Phisik Instrumente tutorial, September 2005.

[6]   I. Hunter and S. Lafontaine, "A Comparison of Muscle with Artificial Actuators," in *Tech. Dig. IEEE Solid State Sensors Actuators Workshop*, 1992, pp 178-185.

[7]   L. Jones, S. Lederman. *Human Hand Function*. Oxford University Press: New York, New York, 2006.

[8]   Beckwith, Marangoni, Lienhard. *Mechanical Measurements*. 5 ed. Addison-Wesley Publishing Company: Reading, Massachusetts, 1993.

[9]   J. Rosmarin and H. Asada. "Synergistic Design of a Humanoid Hand with Hybrid DC motor – SMA Array Actuators Embedded in the Palm." Proceeding of the 2008 IEEE International Conference on Robotics and Automation, 2008.